Society of Petroleum Engineers

SPE-196192-MS

Investigation of Wettability Alteration by Silica Nanoparticles Through Advanced Surface-Wetting Visualization Techniques

Shidong Li, Institute of Chemical and Engineering Sciences, Agency for Science, Technology and Research A*STAR; Daniel Dan, Institute of Materials Research and Engineering, Agency for Science, Technology and Research A*STAR; Hon Chung Lau, Department of Civil and Environmental Engineering, National University of Singapore, Singapore, Singapore. Institute of Chemical and Engineering Sciences, Agency for Science, Technology and Research A*STAR; Nanji J Hadia, Institute of Chemical and Engineering Sciences, Agency for Science, Technology and Research A*STAR; Ole Torsæter, PoreLab, Norwegian Center of Excellence. Department of Geoscience and Petroleum, Norwegian University of Science and Technology NTNU; Ludger P. Stubbs, Institute of Chemical and Engineering Sciences, Agency for Science, Technology and Research A*STAR

This paper was prepared for presentation at the SPE Annual Technical Conference and Exhibition held in Calgary, Alberta, Canada, 30 Sep - 2 October 2019.

Abstract

Altering the wetting state of a rock surface to more water-wet has been proposed as an enhanced oil recovery (EOR) mechanism for nanoparticles. However, how nanoparticles achieve this is not well understood. The objective of this study is to fill this knowledge gap by using advanced 2D and 3D visualization techniques.

In this study, advanced visualization techniques were used to study how hydrophilic silica nanoparticles change the wettability of a glass surface. First, we used interferograms of an oil drop resting on a nanoparticle-treated glass surface to analyze the effect of nanoparticles on wettability. Second, we used Atomic Force Microscopy (AFM) to characterize the structure of nanoparticles covering a glass surface. Third, we used a 2D microfluidic apparatus to visualize wettability alteration caused by the nanoparticle injection. Fourth, we used a fluoresence imaging method with confocal microscopy to find out the reason for this change.

Interferograms of a nanoparticle-treated glass surface showed bright and dark fringes, indicating the presence of a thin water film covering the glass surface caused by nanoparticle adsorption. Furthermore, the higher the nanoparticle concentration, the thicker was the nanoparticle adsorption layer. A low pH environment can reduce nanoparticle adsorption on the glass surface. AFM results showed that the topography of the glass surface changed from smooth to rough after nanoparticle treatment. Microfluidic experiments showed that nanoparticle injection changed the wettability of the grain surface to more water wet. By using a confocal microscopy, we observed a thin water film covering the surface of glass grains suggesting that nanoparticle adsorption is the main mechanism of wettability alteration by nanoparticles.

This paper presents findings of new techniques to study wettability alteration by nanoparticles, including thin-film interferometry, surface characterization by AFM, and fluoresence imaging with confocal

microscopy. Observations showed that nanoparticles adsorption on a glass surface results in a thin water film that prevents the oil from contacting the surface. This is the main mechanism of wettability alteration by nanoparticles. This is the first time use of these advanced visualization techniques to study wettability alteration by nanoparticles is reported.

Introduction

Nanoparticles have been proposed as a cost efficient and environmentally friendly method for EOR [1-3]. Among many EOR mechanisms (interfacial tension reduction [4,5]; wettability alteration [6-8]; disjoining pressure [9,10]; pore channels plugging [11] and emulsification [12]), wettability alteration was suggested as the main one for nanoparticle EOR. However, the mechanism of nanoparticle changing reservoir wettability is not yet well understood, even though many experimental studies have shown the ability of nanoparticles to alter wettability for different substrates and core samples by measuring contact angle and wettability index [14-20]. Better understanding of wettability alteration mechanism of nanoparticle will be helpful for tailoring nanoparticles for EOR.

The wettability of reservoirs plays a critical role in EOR. It can affect the oil-water relative permeability, capillary pressure and residual oil distribution. Changing reservoir wettability to a favorable status will lead to higher oil recovery. Many experimental results using microfluidic observations and corefloods have proven that injection of a nanoparticle suspension, so called nanofluid, can improve oil recovery [21-23]. The effect of nanoparticles on wettability alteration also has been investigated by numerous researchers. Karimi et al., [7] Moghaddam et al. [24] and Monfared et al. [25] reported the effect of different types of nanoparticles (ZrO_2, SiO_2, TiO_2 and $CaCO_3$) on carbonate rock wettability change. All these nanoparticles showed promise on wettability alteration for a carbonate system. They changed carbonate rock from strongly oil wet to strongly water wet. The influence of injection of silica nanoparticle on wettability for oil-wet sandstone rock also showed similar results of changing wettability from oil-wet to strongly water-wet and about 5%-10% additional oil was produced during nanofluid injection [26-28]. Contact angle measurement and wettability index measurement (or spontaneous imbibition) as two commonly used methods, were used in many studies for wettability alteration by nanoparticles. Contact angle measurement results showed a significant contact angle reduction for a substrate after nanoparticle treatment and the equilibrated contact angle was less than 90° [14-15]. Wettability index measurement results showed an overall ability of changing wettability for a core to more water wet regardless if the initial wettability is oil-wet, neutral wet or water wet [17-20]. Moghaddam et al. [24] and Lu et al. [28] reported the effects of wettability alteration by nanoparticles on capillary pressure and oil-water relative permeability, respectively. The results showed that, for a capillary pressure curve, the irreducible water saturation and the entry pressure were increased after nanoparticle treatment. For the oil-water relative permeability curve, the irreducible water saturation and oil-phase relative permeability of the core increased, whereas the water-phase relative permeability decreased.

There are several proposed mechanisms for wettability alteration by nanoparticles. First, Moghaddam et al. [24] discussed the role that structural disjoining pressure plays during wettability alteration. Based on calculation of disjoining pressure of SiO_2 nanoparticles near the vertex, it was shown that the disjoining pressure near the contact line was high enough to advance on the surface and remove the oil from the surface and this is not a slow process. The results also indicated that the smaller nanoparticles size the greater value of disjoining pressure. Second, Monfared et al. [25] reported the responsible mechanism of wettability alteration for the oil-wet calcite surface. They found that the partial release of stearate from the calcite surface and their replacement with silica nanoparticles, and it was verified by surface equilibrium and interaction studies, as well as Fourier transform infrared (FTIR) spectroscopy and field emission scanning electron microscope (FESEM) visualization. They also discussed the role of Na^+ ions in the wettability alteration process. Na^+ ions can assist silica nanoparticle and stearate in adsorption and release, respectively. Third, Ni et al. [26] studied the effect of surface roughness and surface free energy on surface wettability (the

higher the surface roughness and the lower the surface free energy, the more water wet the surface will become). The nanoparticle they used has a micro/nano structure with bead-chain shape, which covered the solid surface and changed the wettability from oil-wet to water-wet. Li et al. [29] also studied the influence of surface roughness on surface wettability by using the Wenzel's model. Their results indicated that the pore wall with nonuniform roughness induced by nanoparticle adsorption is the main mechanism of wettability alteration. Fourth, Lim et al. [13] investigated the correlation between surface volume fraction and surface wettability alteration. They proposed a layering model to explain qualitatively the trend in the change of the solid surface wettability. This indicated the nanoparticle layering near the solid substrate is the main reason for wettability alteration of the solid surface. Fifth, Li et al. [20] proposed a nanoparticle adsorption mechanism for wettability alteration. Due to a large surface area both for nanoparticles and porous media, injection of nanoparticles into porous media will lead to significant adsorption. This adsorption will cover pore wall surface and hence change surface wettability.

In our previous studies [14], we observed a wettability alteration happened in a microfluidic apparatus after nanoparticle injection. The result is shown in Fig. 1. A dark line around the glass grain was found in the microfluidic apparatus after nanoparticle injection, which was not been observed in the microfluidic apparatus without nanoparticles injection. This indicated that the glass surface wettability had been changed from oil-wet (oil can wet the surface completely) to water-wet. We suspected that this change was due to nanoparticle adsorption; hence a thin water film was formed after oil was injected. However, traditional visualization methods could not prove the existence of a water film and explain this phenomenon. So novel surface wetting visualization techniques were utilized in this paper to study the reaction between oil and a substrate surface after nanoparticle treatment. Some new results that could not been observed by using traditional wettability measurement method (contact angle and wettability index) were found and used to explain wettability alteration mechanisms by nanoparticles.

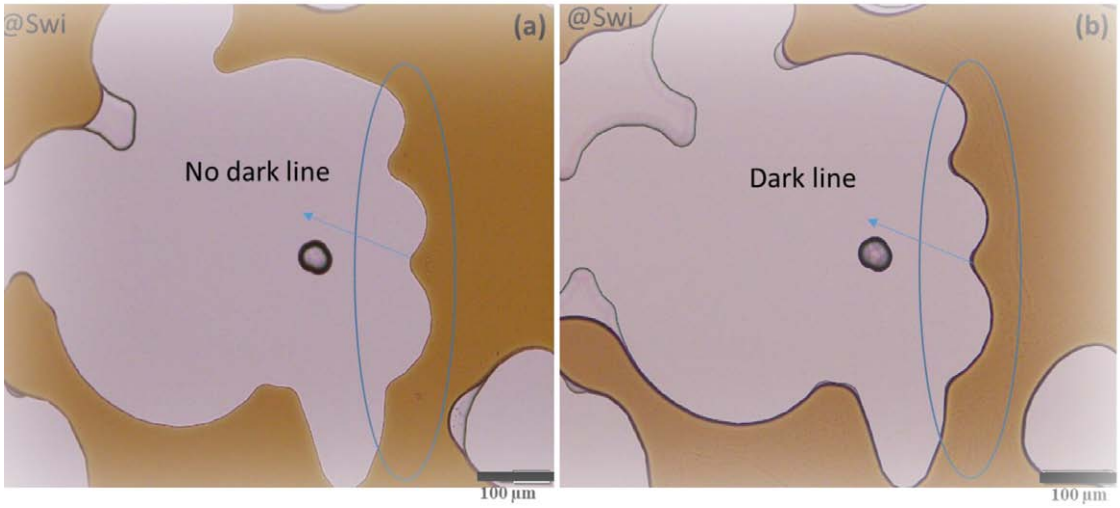

Figure 1—Microscopy images of a microfluidic chip at irreducible water saturation (Swi) [14]. a): without nanoparticle adsorption, b): with nanoparticle adsorption. (modified).

Daniel et al. [30] used the thin-film interference method to study static and dynamic wetting states on a lubricated surface with confocal microscopy. This method confirmed the presence of a stable intercalated lubricant film that repelled a liquid droplet from the solid surface. Atomic force microscopy (AFM) has been utilized to characterize pore wall surface. It can also be used to measure the topography of a substrate surface having a nanoparticle structure on it [31]. Schellenberger et al. [32] used fluoresence 2D/3D imaging technique with confocal microscopy to visualize a liquid droplet on a lubricated surface and studied its

wetting properties. Gong et al. [33] also used this technique to observe the interaction between oil and a microgel and the effect of disjoining pressure on wettability alteration.

In this study, in order to further investigate the mechanism of wettability alteration by nanoparticle, the following experiments were conducted. First, thin-film interference experiments were conducted for glass substrates to study the effect of nanoparticle adsorption on oil wetting status of the surface. The same surface of substrate was characterized with AFM to visualize the nanoparticle structure on it and to measure the surface roughness. We also used fluoresence 2D/3D imaging method to observe the thin water film shown in Fig. 1 and studied wetting state of oil on glass grain surface. By using these novel wetting visualization techniques, some new phenomena of interaction between oil and substrate were observed. They give us a better understanding of the mechanism of wettability alteration by nanoparticles.

Experimental materials and methods

Materials

Hydrophilic silica fumed nanoparticle (FNP) provided by Evonik Industries was used in all experiments. It has an average primary particle size of 7 nm and specific surface area of 300 m^2/g and was characterized with Cryo-Transmission Electron Microscope (Cryo-TEM) and Scanning Electron Microscopy (SEM) (Fig. 2). Limonene (purity of 96%) was purchased from Fisher Scientific. Rhodamine 6G (R6), Nile Red (NR) and silicon oil were purchased from Sigma-Aldrich. All reagents were used as received. Deionized water with a resistivity of 17MΩcm was used as the aqueous phase.

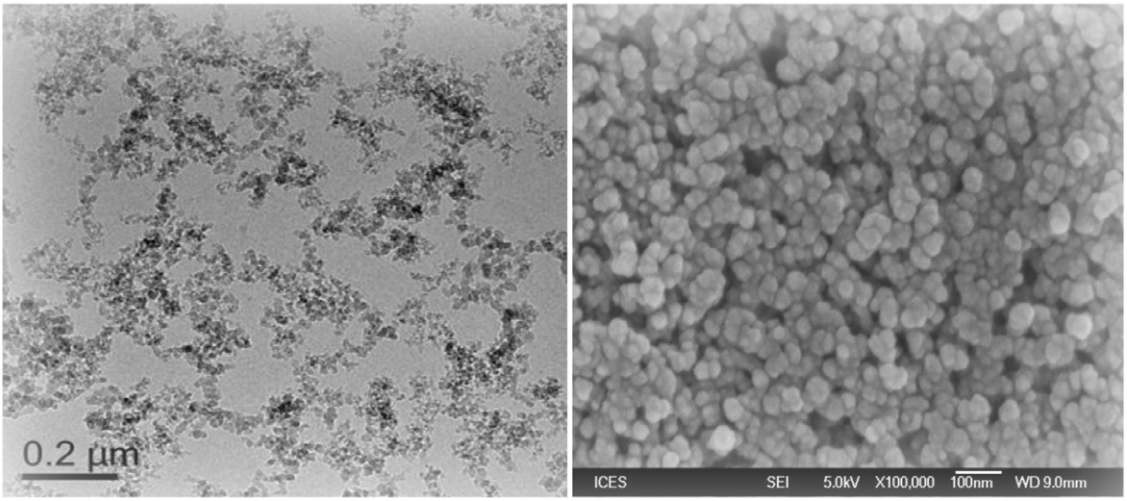

Figure 2—Cryo-TEM image (left) and SEM image (right) of FNP

Substrate and microfluidic devices

Glass chips (1.5 cmx1.0 cm) cut from a microscope slide were used as a substrate in this study. Two substrates soaked in nanofluid/brine were prepared for thin-film interferometry and AFM experiment. The microfluidic chip purchased from Micronit Micro Technologies was used. This microfluidic chip was manufactured based on the pore structure of a two-dimensional physical rock. The pore structure was etched onto the surface of a flat glass plate, which was covered by another glass plate, thus creating an enclosed pore space. Pore structure and parameters of the microfluidic chip are shown in Fig. 3 and Table 4. Since the pore structure was etched with hydrofluoric acid the wettability of this microfluidic chip was oil wet [34].

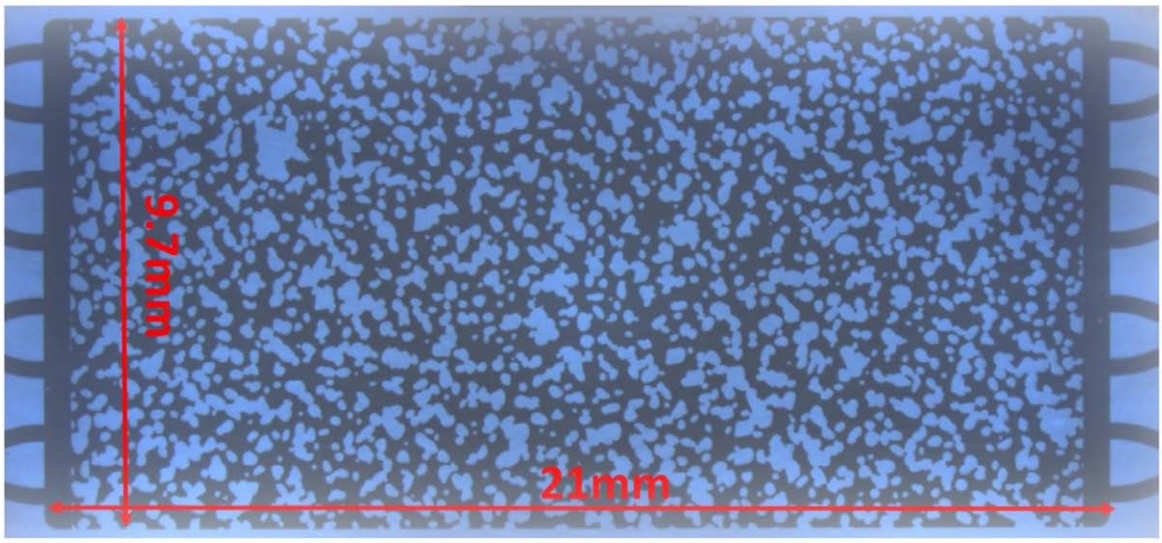

Figure 3—Microfluidic pore structure image. Brown and white colors represent pore volume and grain volume, respectively.

Preparation of nanofluid

Three nanoparticle concentrations (0.05, 0.1 and 0.5 wt. %) were used in this study. A 3 wt. % NaCl brine was used as dispersion fluid for FNP. For nanofluid preparation, solid powder nanoparticles were weighted and dispersed in brine by using sonicator. The pH of some nanofluid was reduced by addition of hydrochloric acid (HCl).

Thin-film interference experiment

The thin-film interference experiment for the substrate soaked in nanofluid/brine was performed using a confocal laser scanning microscope (CLSM). The schematic of the setup is shown in Fig. 4. A silicon oil droplet was placed above the glass substrate, so that it just touched the substrate surface. The whole setup was put inside a petri dish, which was filled with brine. During the experiment we raster scanned the surface of substrate with one focused beam of monochromatic light with wavelength λ=561 nm, and captured the reflected light through the pinhole of a confocal microscope; Thus, only reflected light from the focal plane, that was, the interface of interest, was able to reach the photomultiplier tube of the microscope [30]. In the presence of a thin water film, the light reflected off the solid/water and water/oil droplet interfaces would interfere with one another constructively or destructively to give bright or dark fringes, respectively. We can get the oil wetting status of the surface by analyzing the interferograms for the cases with and without nanoparticle adsorption.

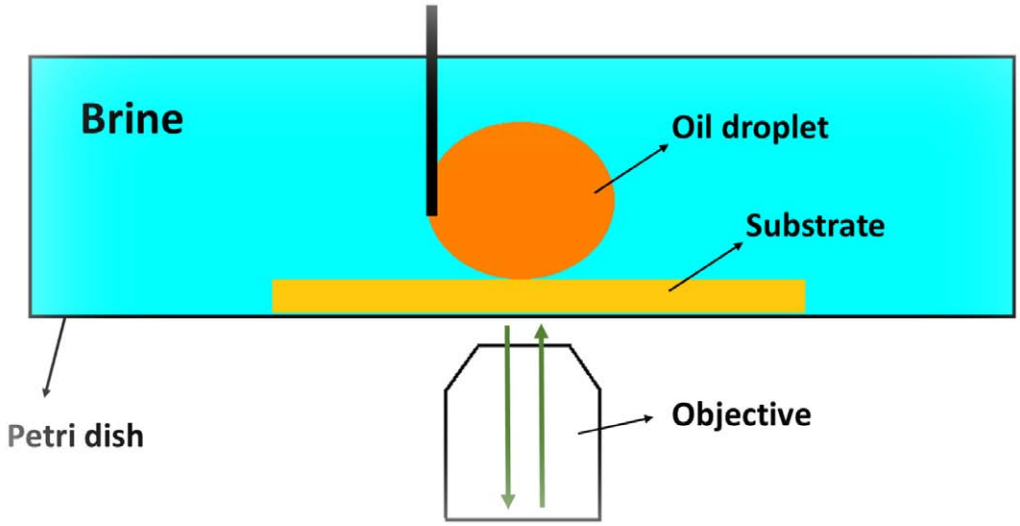

Figure 4—Schematic of setup of thin-film interference experiment

AFM topography measurement

AFM topography measurement was conducted on another glass substrate soaked in nanofluid/brine. In order to get comparable results, all AFM measurements were performed in brine, and the measured field area was 10 μm x10 μm.

Table 1—Microfluidic chip parameters

Parameters	Value
Total chip thickness	1800 μm
Chip size	45 mm × 15 mm
Rockpore volume	2.3 μl
Porosity	0.57
Permeability	2.5 Darcy

Fluoresence imaging microscopy of microfluidic

Before conducting the fluoresence imaging for the microfluidic chip, brine and limonene mixed with fluorescent dye were injected into it. Limonene was selected as the oleic phase due to its nonpolarity. Fluorescent dyes of R6 and NR was added into brine and limonene, respectively. The injection process followed the protocol described in the following. First, the microfluidic chip was vacuumed and saturated with brine completely, and then brine was injected at a flow rate of 0.01ml/min for about 10 minutes. For the microfluidic chip treated with nanoparticles, prior to injection of brine with R6, nanofluid was injected at a flow rate of 0.01ml/min for about 60 minutes to allow sufficient nanoparticle adsorption on glass grains. Next, 30 minutes of brine injection with R6 was followed at a 0.01ml/min flow rate, allowing the fluorescent dye R6 to mix with nanoparticle adsorption structure. Finally the limonene with NR was injected to displace the brine out at a flow rate of 0.0005 ml/min for 60 minutes. Afterwards, the inlet and outlet of the microfluidic chip were blocked to prevent liquid evaporation. A new microfluidic chip was used for each flooding experiment to ensure the same initial condition.

Then the microfluidic chip was fixed on the sample stage of CLSM. During fluoresence imaging microscopy, the dye of NR in the oleic phase (limonene) was excited using a 561nm laser and the emission was detected from 570 to 620 nm. The dye of R6 in the aqueous phase (brine) was excited by using a 488

nm laser and the emission was detected from 500 to 550 nm. Both 2D and 3D images of microfluidic chip were acquired to study the mechanism of wettability alteration by nanoparticles.

Results and Discussion

Thin-film interference experiments

In order to prove the thin-film interference experiment was suitable for surface wetting study, first we conducted an experiment with a blank substrate and the substrate soaked in nanofluid (with nanoparticles adsorption), and the results are shown in Fig. 5. It shows a significant difference of interferograms between the substrate with and without nanoparticle adsorption. In Fig. 5c, the contact area with oil is black without any fringes. The reason might be due to partially hydrophobic surface of the glass substrate, so oil droplet was able to touch the surface and the water in between was drained out. When laser shone to the substrate only the light from solid and oil interface was reflected back to the objective (Fig. 5a). Hence the interference did not happen. Fig. 5c also shows a bigger contact area with oil droplet indicating a greater contact angle value. However, for the substrate with nanoparticle adsorption, Fig. 5d shows an interferogram with clear bright and dark fringes, which proves the existence of a thin water film between the oil droplet and substrate surface. Nanoparticles adsorbed on the substrate surface formed a nano-structure (nanoparticle cluster shown as circle spots in Fig. 5d) due to their surface area and surface charge. When the surface is touched by the oil droplet, water can be trapped inside these nano-structures due to capillary pressure and form a thin water film preventing the surface from wetting by oil. So when a laser shone to the surface with nanoparticle adsorption, two lights reflected off the solid/water and water/oil interface interfered with one another. The bright and dark fringes formed due to constructive and destructive interference. The contact area with oil droplet of the substrate is smaller indicating a smaller contact angle.

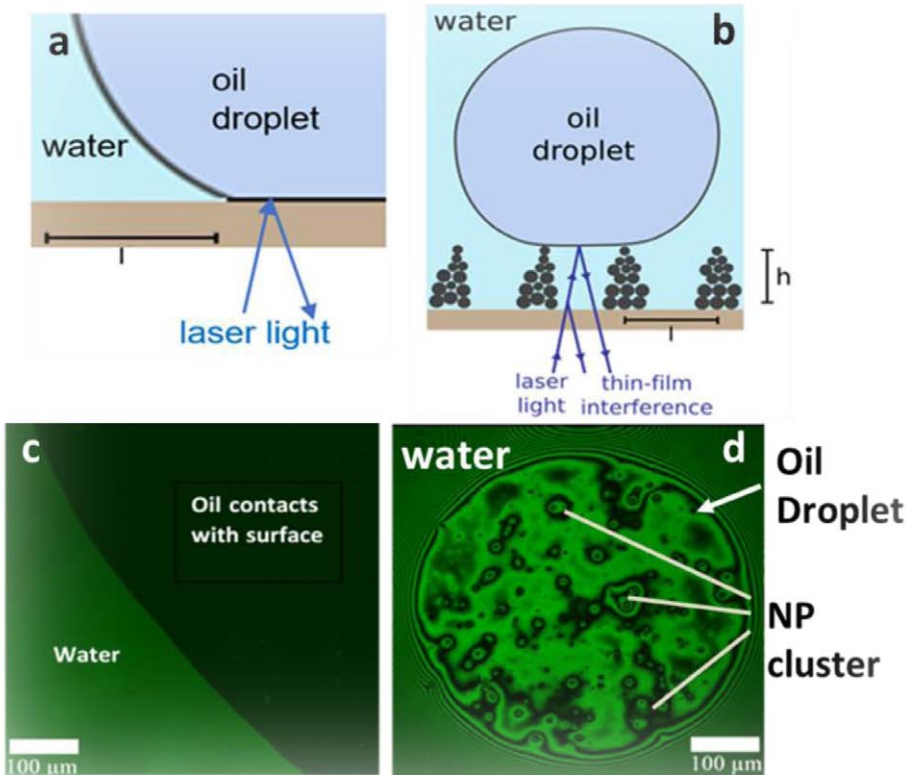

Figure 5—Thin-film interference experiment. a) Schematic representing the substrate without nanoparticles adsorption. b) Schematic representing the thin-film interference effects due to the thin water film. c) Image of oil contact area for the surface without nanoparticle adsorption. d) Interferogram of the surface with nanoparticle adsorption.

Figure 6 shows the interferograms for the substrates treated with nanofluids with three different concentrations (0.02, 0.1 and 0.5 wt. %). There is a significant difference among these three cases. Bright and dark fringes became denser with increase in nanoparticle concentration. This might be due to more nanoparticle adsorption in a nanofluid with higher concentration. In Fig. 6a, there are only few visible nanoparticle clusters, while Fig. 6b has more nanoparticle clusters and Fig. 6c has the most nanoparticle cluster, which lead to highly dense fringes. Since the laser's wavelength is constant, the distance between bright and dark fringes next each other is also constant and the value is half of the wavelength (λ=561 nm). Hence, the denser and the more concentrated fringes, the thicker is nanoparticle adsorption. Thicker adsorption results in less contact area with oil, hence leading to a smaller contact angle. This result is consistent with our previous study of contact angle measurement for the same substrate treated with nanoparticles.

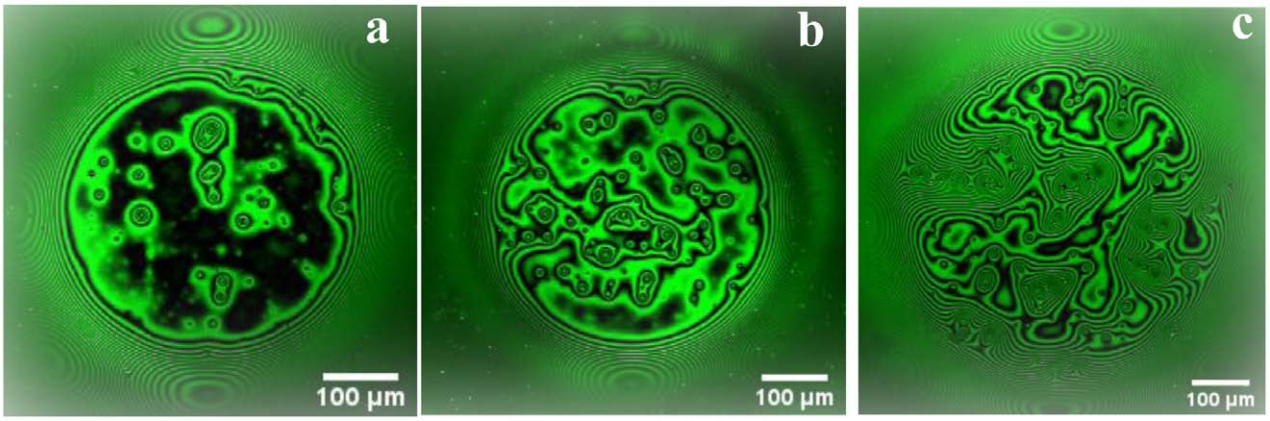

Figure 6—Interferogram of the substrate soaked in nanofluid with different nanoparticle concentration. a) 0.02 wt. %. b) 0.1 wt. %. c) 0.5 wt. %.

The effect of low pH on nanoparticle adsorption on substrate was investigated and the results are shown in Fig. 7. The pH of 0.1 wt. % nanofluid is about 4.84, and the pH of other two nanofluid samples was adjusted to 3.03 and 2.01 by addition of HCl, respectively. In Fig. 7b-c, the nanoparticle clusters are fewer and fringes are thinner than those in Fig. 7a. Based on the same theory mentioned above, we can conclude that a low pH can reduce nanoparticle adsorption on the surface. Since glass substrate is a composite of silica, this can be explained with "H^+ protection theory" [35]. Even through the nanoparticle adsorption is thinner, the nano-structure formed is still effective in repelling oil from wetting the substrate and thus create a smaller contact angle.

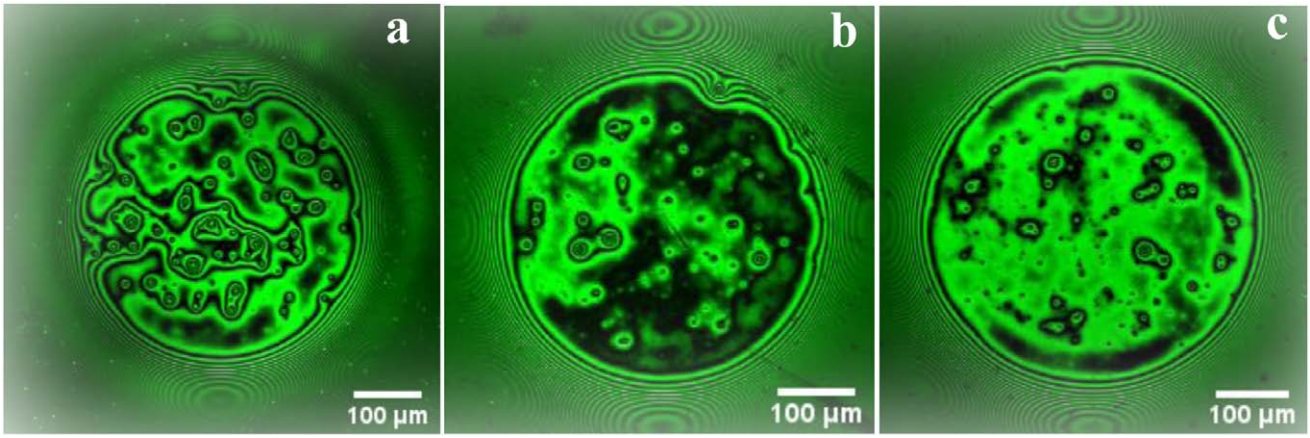

Figure 7—Interferogram for the surface of substrate soaked in naofluid with 0.1 wt. % nanoparticle but different pH. a) pH=4.84. b) pH=3.03. c) pH=2.01.

AFM experiments

The topography of the substrate surface treated with nanoparticles was characterized with AFM. These substrates were soaked in the nanofluids together with the substrates used in previous experiments in the same batch. The topography images and surface roughness data of the substrates treated with nanofluids with different concentrations are shown in Fig. 8 and Table 2, respectively. The surface of a blank substrate without nanoparticles adsorption was very smooth (Fig. 8a). The average roughness was only 1.711 nm. However, the surface of substrates became rougher when they were treated with the nanofluid and the surface roughness increased to about 37.48 nm for 0.5 wt. % case. More significant nanoparticle clusters with a height more than 100 nm (white spots in Fig. 8c and 8d) adsorbed on the surface were observed. The substrate treated with 0.5 wt. % (Fig. 8d) has more nanoparticle clusters and thicker nanoparticles adsorption than the one treated with 0.1 wt. % (Fig. 8c). This is consistent with the conclusions drawn in the previous section. Water can be trapped within these nano-structures when the surface was contacted by an oil droplet.

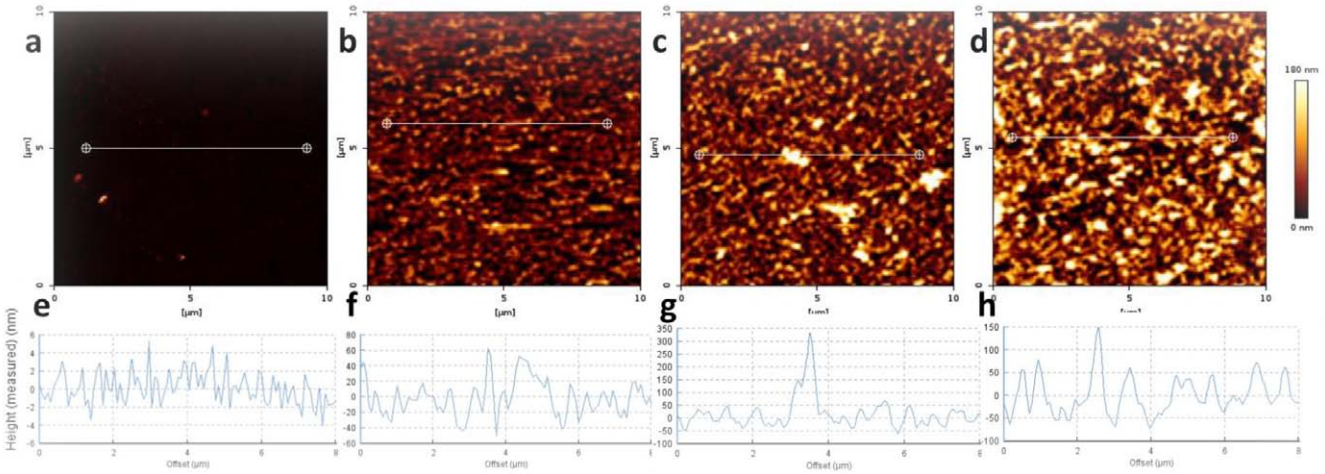

Figure 8—AFM topography image of the substrate soaked in nanofluids with different nanoparticle concentration. a) blank substrate. b) 0.02 wt. %. c) 0.1 wt. %. d) 0.5 wt. %. e, f, g and h are surface height along the white lines in a, b, c and d, respectively.

Table 2—Surface roughness of the substrate soaked in nanofluids with different nanoparticle concentration

NP concentration	0	0.02 wt. %	0.1 wt. %	0.5 wt. %
Average Roughness	1.711 nm	18.61 nm	25.93 nm	37.48 nm
Root Mean Square Roughness	3.502 nm	23.87 nm	35.62 nm	48.82 nm
Peak-to-Valley Roughness	6.514 nm	246.7 nm	420.6 nm	432.3 nm

The effect of a low pH (pH= 3.03 and 2.01) environments on topography of a surface treated with nanoparticles was also studied with AFM and the results are shown in Fig. 9 and Table 3. By analyzing the images with surface height (Fig. 9a, b, c) and the surface roughness data (Table 4) of the three substrates, we may conclude that there was no significant difference on surface roughness and adorption thickness between higher pH and lower pH cases. Howerer, a low pH environment increased the homogeneity of nanoparticle adsorption and reduces significant nanoparticle clusters on the surface. The value of peak to valley roughness decreased from 420.6 nm (pH=4.48) to 319.0 nm (pH=2.01). A uniform nanoparticle adsorption on substrate surface is helpful for wettability alteration and can eliminate pore channels plugging by nanoparticle in a porous medium.

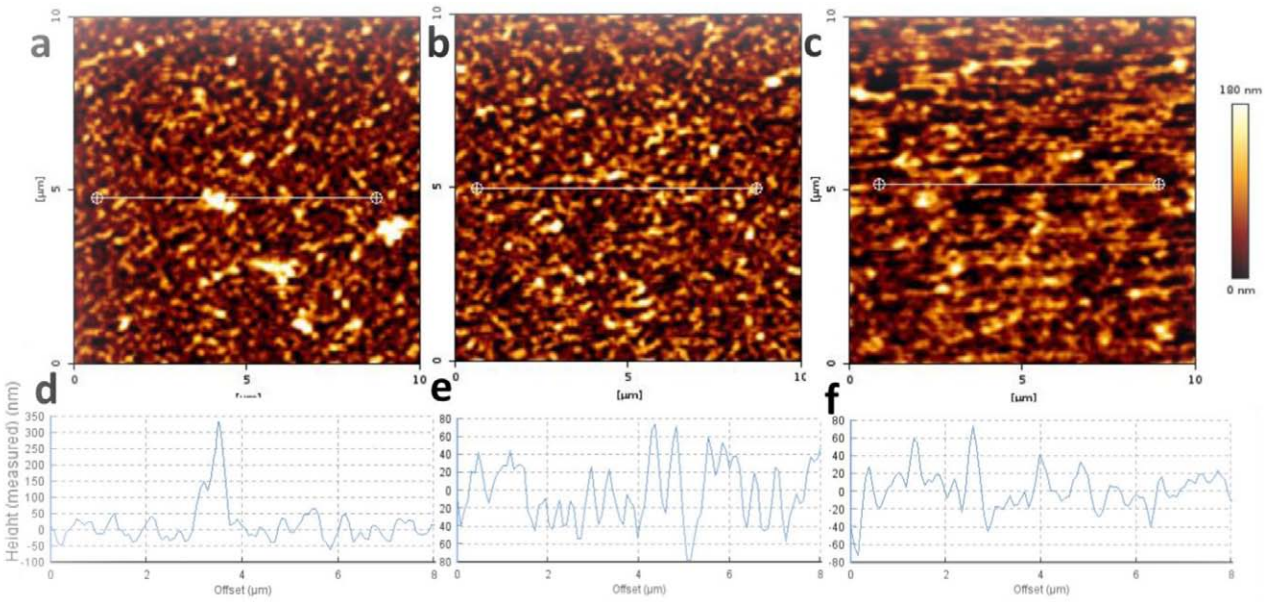

Figure 9—AFM topography image of the substrate soaked in nanofluid with nanoparticle concentration 0.1 wt. % but different pH. a) 4.84. b) 3.03. c) 2.01. d, e and f are surface height along the white line in a, b and c, respectively.

Table 3—Surface roughness of the substrate soaked in nanofluid with 0.1 wt. % nanoparticle concentration but different pH.

pH	4.84	3.03	2.01
Average Roughness	25.93 nm	27.53 nm	28.12 nm
Root Mean Square Roughness	35.62 nm	35.67 nm	35.87nm
Peak-to-Valley Roughness	420.6 nm	353.6 nm	319.0 nm

A 3D topography image of the substrate treated with 0.1 wt. % nanofluid is shown in Fig. 10. It shows nanoparticle adsorption is heterogeneous with different height.

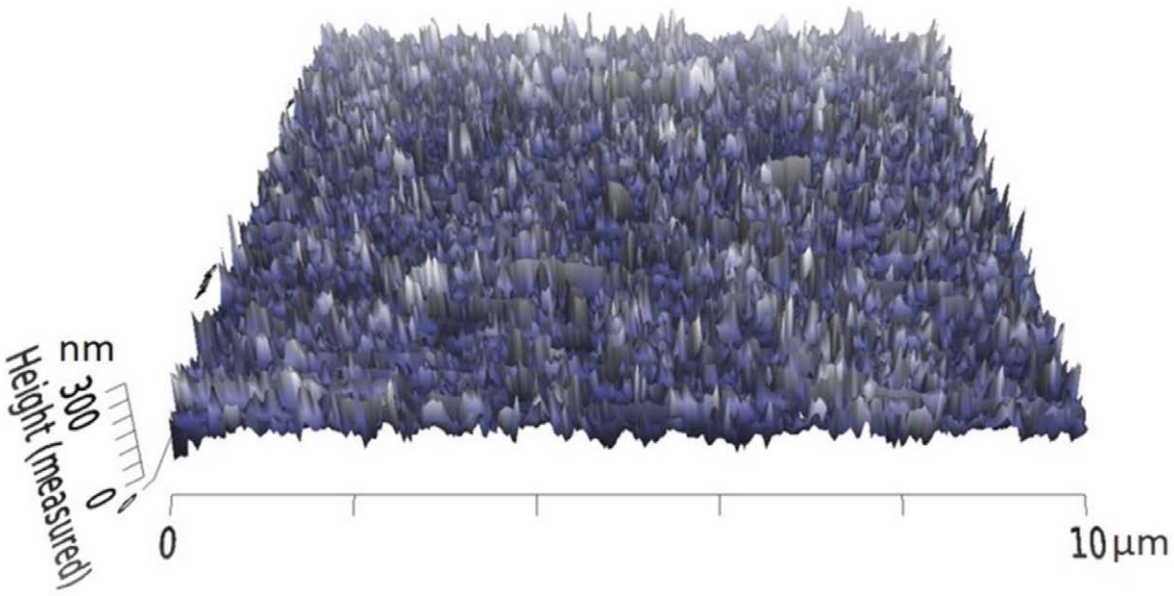

Figure 10—3D topography for the surface of substrate soaked in 0.1 wt. % nanoparticles, pH=4.84.

Fluoresence imaging experiments with microfluidic

Fluoresence imaging with CLSM technique was used for the microfluidic study. Brine and silicon oil with different fluorescent dyes were injected into the microfluidic chip and light with different wavelength was emitted under the shining of lasers. Hence, we can distinguish the aqueous phase from the oleic phase and observe their reactions with glass grains (glass grains were always shown in black, since glass does not fluoresce).

The images of the same region in microfluidics with and without nanoparticle treatment are shown in Fig. 11. Similar to Fig. 1a, the oil (red) in the microfluidic chips without nanoparticles treatment contacted with glass grains and the dye of NR adsorbed on grains surface and formed some "red rings." Since the NR only dissolves in oleic phase, so it can be proven that oil touched the grains directly and water was drained out during oil injection process indicating the oil-wet wetting state of glass grains. The residual brine (green) in Fig. 11a was trapped in pores during oil injection. Fig. 11b shows the image for the microfluidic chip with nanofluid injection before drainage process. There is a clear difference compared to the one in Fig. 11a. Oil in red was no longer in contact with glass grains and a thin film in green was always observed between oil and grains. Since the R6 only dissolves in water, it can be concluded that a thin water film can be formed on the surface of glass grains after injection of nanofluid. This can prevent grain surface from wetting by oil. Figure 11c shows the image for the microfluidic chip injected with nanofluid with a pH of 2.01. As described in previous sections, a low pH environment affects nanoparticle adsorption. However, it does not affect the formation of a thin water film in the microfluidic chip. This suggests a promising potential for wettability alteration application. The color of oil in the three images varied from dark red (Fig. 11a) to light red (Fig. 11b). The reason for this phenomenon is nanoparticle adsorption on upper and lower glass plates of the microfluidic chip. Hence the thickness of pore channel was reduced. So oil thickness is smaller in Figs. 11 b and c. Oil emitted different light under the same setting of excitation and emission.

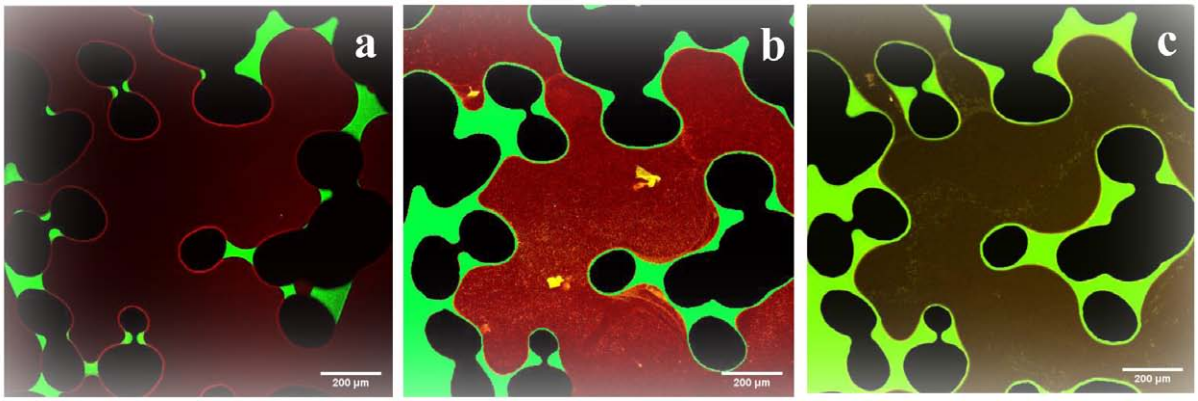

Figure 11—Fluorescent microscopy images of microfluidics chips (red: oil; green: brine; black: glass grains). a) without nanoparticle adsorption. b) treated with 0.1 wt.% nanofluid pH=4.84. c) treated with 0.1 wt. % nanofluid pH=2.01.

It is possible to a capture 3D image by using CLSM, which is helpful to study microfluidic flow in 3D, even though microfluidic is considered as a 2D model. The 3D images of the microfluidics chips treated with and without nanoparticles are shown in Fig. 12. The thickness of the pore structure is about 20 µm. The images with cross section fluid type information along the yellow lines for the microfluidic chips treated with and without nanoparticles are shown in Fig.13. The same location of grain surface from two microfluidics was selected as cross point, and the information of fluid type is shown in white circles.

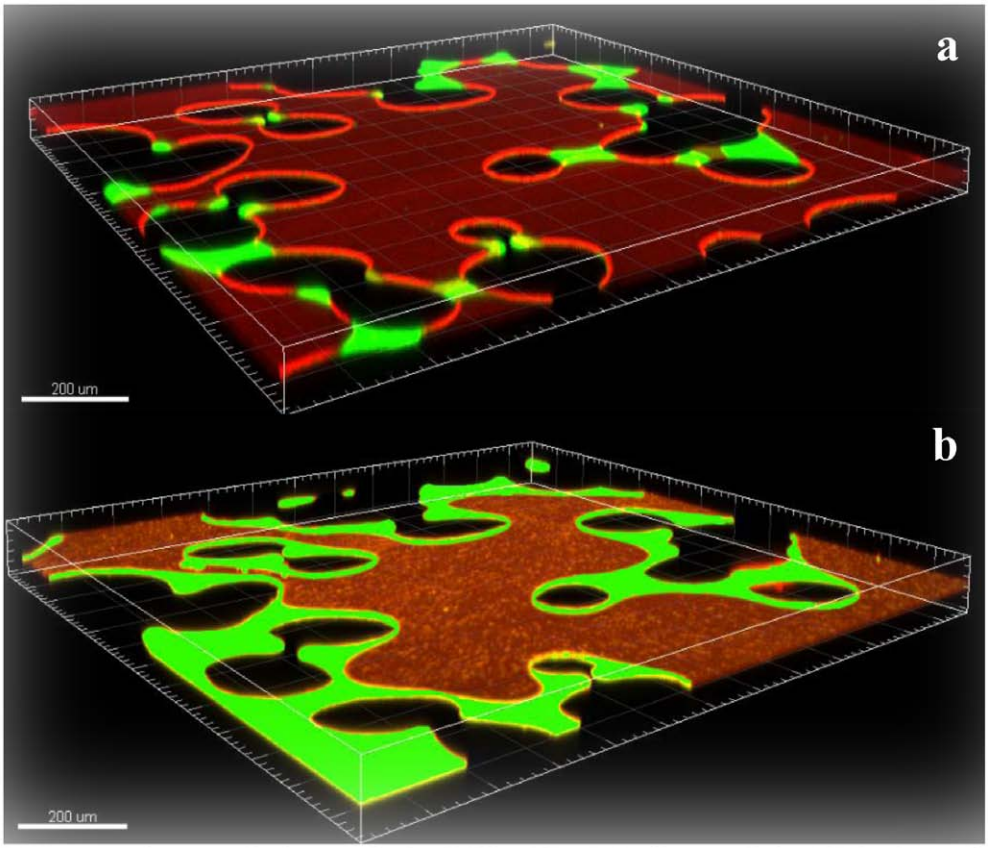

Figure 12—Fluorescent microscopy 3D images of microfluidics chips (red: oil; green: brine; black: glass grains). A) Microfluidic chip without nanoparticle adsorption. b) Microfluidic chip treated with nanofluid pH=2.01.

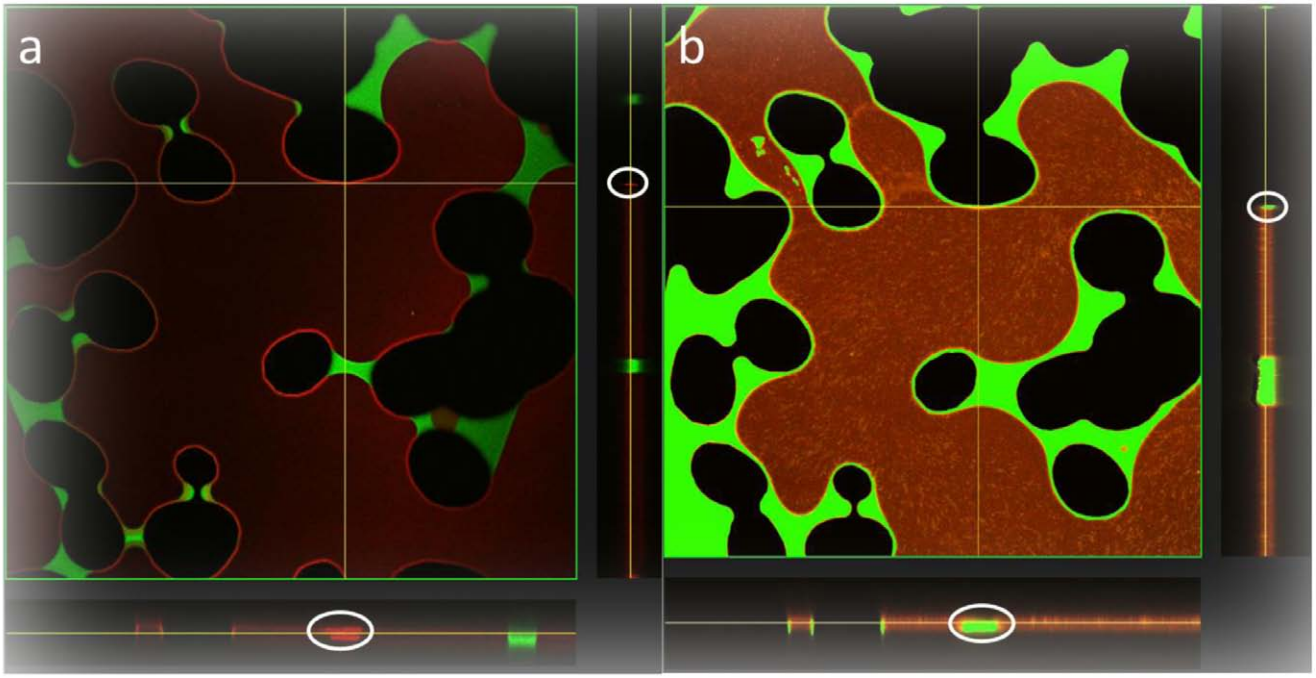

Figure 13—Fluorescent microscopy images of microfluidics chips with cross section fluid information along the yellow lines (red: oil; green: brine; black: glass grains). a) Microfluidic chip without nanoparticle adsorption. b) Microfluidic chip treated with nanofluid pH=2.01.

It can be seen that, in 3D, the fluid contacting the grain surface in Fig. 13a is oil, whereas the fluid contacting the grain surface in Fig. 13b is brine. This is evidence to prove the existence of a thin water film on the grain surface after nanoparticle injection. The dark lines around grain surface in Fig. 1b can be proven as thin water films. The results of fluoresence imaging experiments with the microfluidic chips show that nanoparticle adsorption is the main mechanism for wettability alteration by nanoparticles.

Conclusions

In this work, we used advanced surface wetting visualization techniques (thin-film interferometry, AFM topography measurement and fluoresence imaging with CLSM for microfluidic) to study the effect of nanoparticle adsorption on wettability alteration. Based on visualization results, the following conclusions can be drawn.

1. Thin-film interferometry can be used for wettability alteration study and shows more details of interaction between oil and a substrate surface. Both nanoparticle concentration and a low pH environment can affect nanoparticle adsorption on the surface and hence the wettability. The higher the nanoparticle concentration, the thicker is the nanoparticle adsorption and the more water-wet the surface becomes. The lower the pH of nanofluid, the less nanoparticles adsorb on the surface. However, it is still sufficient to change wettability to more water-wet.
2. Topography and surface roughness of the surface can be measured with AFM for the substrate treated with nanoparticles. The higher the nanoparticle concentration, the more nanoparticle adsorbs on the surface and the rougher surface becomes. A low pH environment has no significant effect on the thickness of nanoparticle adsorption and surface roughness of the surface. However, a low pH environment favors uniform nanoparticle adsorption.
3. The fluoresence imaging technique with CLSM is a promising method to visualize oil-water distribution and oil-grain interaction in a microfluidic chips. Both 2D and 3D images proved that a layer of nanoparticle was adsorbed on the grain surface during nanofluid injection, and a thin

water film was formed during the oil drainage process. This thin water film prevented the grain surface from wetting by oil. This indicates that the wettability surface of microfluidic has been changed from oil-wet to water-wet.

Acknowledgment

We thank SNG Anqi for performing AFM measurement. The work was supported by the Science and Engineering Research Council (SERC), A*STAR, Singapore.

1. Kong, X. and Ohadi, M.M. *Applications of Micro and Nano Technologies in the Oil and Gas Industry - Overview of the Recent Progress*. Paper SPE 138241-MS presented at Abu Dhabi International Petroleum Exhibition and Conference, 1-4 November 2010, Abu Dhabi, UAE.
2. Lau, H. C., Yu, M., and Nguyen, U. P. 2016. Nanotechnology for oilfield Applications: Challenges and impact. Presented at the Abu Dhabi International Petroleum Exhibition & Conference, 7-10 November 2016, Abu Dhabi, UAE.
3. Li, S., Hendraningrat, L. and Torsater, O. 2013. Improved oil recovery by hydrophilic silica nanoparticles suspension: 2-phase flow experimental studies. Presented at the International Petroleum Technology Conference, 26-28 March 2013, Beijing, China.
4. Joonaki, E. and Ghanaatian, S. 2014. The Application of Nanofluids for Enhanced Oil Recovery: Effects on Interfacial Tension and Coreflooding Process. *Petroleum Science and Technology*. **32**, 2599-2607.
5. Moradi, B., Pourafshary, P., Jalali, F., Mohammadi, M. and Emadi, M. A. 2015. Experimental Study of Water-based Nanofluid Alternating Gas Injection as a Novel Enhanced Oil Recovery Method in Oil-wet Carbonate. *Journal of Natural Gas Science and Engineering*. **27**. 64-73.
6. Li, S., Kaasa, A. T., Hendraningrat, L. and Torsæter. O. Effect of Silica Nanoparticles Adsorption on the Wettability Index of Berea Sandstone. Presented at the International Symposium of the Society of Core Analysts, 16-19 September, 2013, Napa Valley, California, USA.
7. Karimi, A., Fakhroueian, Z., Bahramian, A., Khiabani, N., Darabad, J., Azin, R. and Arya, S. Wettability Alteration in Carbonates using Zirconium Oxide Nanofluids: EOR Implications. *Energy Fuels*. 2012, **26**, 1028-1036.
8. Maghzi, A., Mohammadi, S., Ghazanfari, M. H., Kharrat, R. and Masihi, M. Monitoring wettability alteration by silica nanoparticles during water flooding to heavy oils in five-spot systems: A pore-level investigation. *Experimental Thermal and Fluid Science* Volume **40**, July 2012, Pages 168-176.
9. Wasan, D.T. and Nikolov, A. 2003. Spreading of nanofluids on solids. *Journal of Nature* **423** (8 May): 156-159.
10. Wasan, D.T., Nikolov, A. and Kondiparty, K. 2011. The wetting and spreading of nanofluids on solids: Role of the structural disjoining pressure. *Current Opinion in Colloid & Interface Science* **16** (4): 344-349.
11. Hendraningrat, L., Li, S., Suwarno. and T orsæter. O. A Glass Micromodel Experimental Study of Hydrophilic Nanoparticles Retention for EOR Project. Presented at the SPE Russian Oil and Gas Exploration and Production Technical Conference and Exhibition, 16-18 October, 2012, Moscow, Russia.
12. Zhang, T., Roberts, M. R., Bryant, S. L. and Huh, C. 2009. Foams and Emulsions Stabilized With Nanoparticles for Potential Conformance Control Applications. Presented at the 2009 SPE International Symposium on Oilfield Chemistry held in The Woodlands, Texas, USA, 20–22 April.

13. Lim, S., Horiuchi, H. Nikolov, A. D. and Wasan, D. Nanofluids Alter the Surface Wettability of Solids. *Langmuir* 2015, **31**, 5827-5835.
14. Li, S., Hadia, N. J., Lau, H. C., Torsaeter, O., Stubbs, L. P. and Ng, Q. H. 2018. Silica Nanoparticles Suspension for Enhanced Oil Recovery: Stability Behavior and Flow Visualization. Presented at the SPE Europec featured at the 80th EAGE Conference and Exhibition, Copenhagen, Denmark, 11-14 June.
15. Bayet, A. E., Junin, R., Samsuri, A., Piroozian, A. and Hokmabadi, M. 2014. Impact of Metal Oxide Nanoparticles on Enhanced Oil Recovery from Limestone Media at Several Temperatures. *Energy & Fuels*, **28**, 6255-6266.
16. Jiang, R., Li, K., and Horne, R., 2017. A Mechanism Study of Wettability and Interfacial Tension for EOR Using Silica Nanoparticles. Presented at the SPE Annual Technical Conference and Exhibition held in San Antonio, Texas, USA, 9-11 October.
17. Li, S., Torsaeter, O., Lau, H. C., Hadia, N. J. and Stubbs, L. P. The Impact of Nanoparticle Adsorption on Transport and Wettability Alteration in Water-Wet Berea Sandstone: An Experimental Study. *Front. Phys*, 2019, Volume **7**, Article 74,
18. Li, S. and Torsaeter, O. 2015. The Impact of Nanoparticles Adsorption and Transport on Wettability Alteration of Intermediate Wet Berea Sandstone. Presented at the SPE Middle East Unconventional Resources Conference and Exhibition, Muscat, Oman, 26-28 January.
19. Li, S. and Torsaeter, O. 2015. The Impact of Nanoparticles Adsorption and Transport on Wettability Alteration of Water Wet Berea Sandstone. Presented at the SPE/IATMI Asia Pacific Oil & Gas Conference and Exhibition, Nusa Dua, Bali, Indonesia, 20-22 October.
20. Li, S. and Torsaeter, O. 2015. Experimental Investigation of the Influence of Nanoparticles Adsorption and Transport on Wettability Alteration for Oil Wet Berea Sandstone. Presented at the SPE Middle East Oil & Gas Show and Conference, Manama, Bahrain, 8-11 March.
21. Li, S. and Torsaeter, O. 2014. An Experimental Investigation of EOR Mechanisms for Nanoparticles Fluid in Glass Micromodel. at the International Symposium of the Society of Core Analysts September, 2014, Avignon, France.
22. Hendraningrat, L., Li, S. and Torsæter. O. A coreflood investigation of nanofluid enhanced oil recovery. *Journal of Petroleum Science and Engineering*. Volume **111**, November 2013, Pages 128-138
23. Kanj, M. Y., Funk, J. J. and Al-Yousif, Z. 2009. Nanofluid Coreflood Experiments in the ARAB-D. Presented at the SPE Saudi Arabia Section Technical Symposium, 9-11 May 2009, Al-Khobar, Saudi Arabia.
24. Moghaddam, R. N., Bahramian, A., Fakhroueian, Z., Karimi, A. and Sharareh, A. Comparative Study of Using Nanoparticles for Enhanced Oil Recovery: Wettability Alteration of Carbonate Rocks. *Energy Fuels* 2015, **29**, 4, 2111-2119.
25. Monfared, A. D., Ghazanfari, M. H., Jamialahmadi, M. and Helalizadeh, A. Potential Application of Silica Nanoparticles for Wettability Alteration of Oil–Wet Calcite: A Mechanistic Study. *Energy Fuels* 2016, **30**, 5, 3947-3961.
26. Ni, X., Jiang, G., Liu, F., and Deng Z. Synthesis of an Amphiphobic Nanofluid with a Novel Structure and Its Wettability Alteration on Low-Permeability Sandstone Reservoirs. *Energy Fuels* 2018, **32**, 4, 4747-4753.
27. Giraldo, J., Benjumea, P., Lopera, S., Cortés, F. B. and Ruiz, M. A. Wettability Alteration of Sandstone Cores by Alumina-Based Nanofluids. *Energy Fuels* 2013, **27**, 7, 3659-3665.
28. Lu, T., Li, Z. Zhou, Y. and Zhang, C. Enhanced Oil Recovery of Low-Permeability Cores by SiO2 Nanofluid. *Energy Fuels* 2017, **31**, 5, 5612-5621.

29. Li, R., Jiang, P., Gao,C., Huang, F., Xu, R. and Chen, X. Experimental Investigation of Silica-Based Nanofluid Enhanced Oil Recovery: The Effect of Wettability Alteration. *Energy Fuels* 2017,**3**,11,188-197
30. Daniel, D., Timonen, J. V. I., Li, R., Velling, S. J. and Aizenberg, J. Oleoplaning droplets on lubricated surfaces. *Nature Physics*, 2017, Volume **13**, Number 10, Page 1020.
31. Javadpour, F., Farshi, M. M. and Amrein M. Atomic-Force Microscopy: A New Tool for Gas-Shale Characterization. *Journal of Canadian Petroleum Technology*. 2012, 51-04.
32. Schellenberger, F., Xie, J., Encinas, N., Hardy, A., Klapper, M., Papadopoulos, P., Butt, H. J. and Vollmer, D. Direct observation of drops on slippery lubricant-infused surfaces. *Soft Matter*, 2015, **11**, 7617-7626.
33. Gong, Y., Wang, M., Zhang, Z. and He, J. Microgel evolution at three-phase contact region and associated wettability alteration. *Colloids and Surfaces A*. **558** (2018) 297–302.
34. Ramakrishnaiah, R., Alkheraif, A. A., Divakar, D. D., Matinlinna, J. P. and Vallittu, P. K. The Effect of Hydrofluoric Acid Etching Duration on the Surface Micromorphology, Roughness, and Wettability of Dental Ceramics. *Int. J. Mol. Sci* 2016, **17**(6), 822.
35. Sofla, S. J.D., James, L. A. and Zhang, Y. Insight into the stability of hydrophilic silica nanoparticles in seawater for Enhanced oil recovery implications. *Fuel*, Volume **216**, 15 March 2018, Pages 559-571